

## Supplementary Information for

### **An air/metal hydride battery for simultaneous neutralization treatment of acid-base wastewater and power generation**

Kangqiang Ye<sup>1,2</sup>, Yu'an Du<sup>1</sup>, Yuxin Yang<sup>1</sup>, Rong Chen<sup>1</sup>, Chao Deng<sup>1,\*</sup>, Guo-Ming Weng<sup>1,\*</sup>

<sup>1</sup> Shanghai Key Laboratory of Hydrogen Science & Center of Hydrogen Science, School of Materials Science and Engineering, Shanghai Jiao Tong University, Shanghai 200240 P. R. China

<sup>2</sup> Department of Mechanical Engineering, The University of Hong Kong, Pokfulam Road, Hong Kong SAR, China

\*Corresponding authors.

E-mail: chaodeng@sjtu.edu.cn; guoming.weng@sjtu.edu.cn

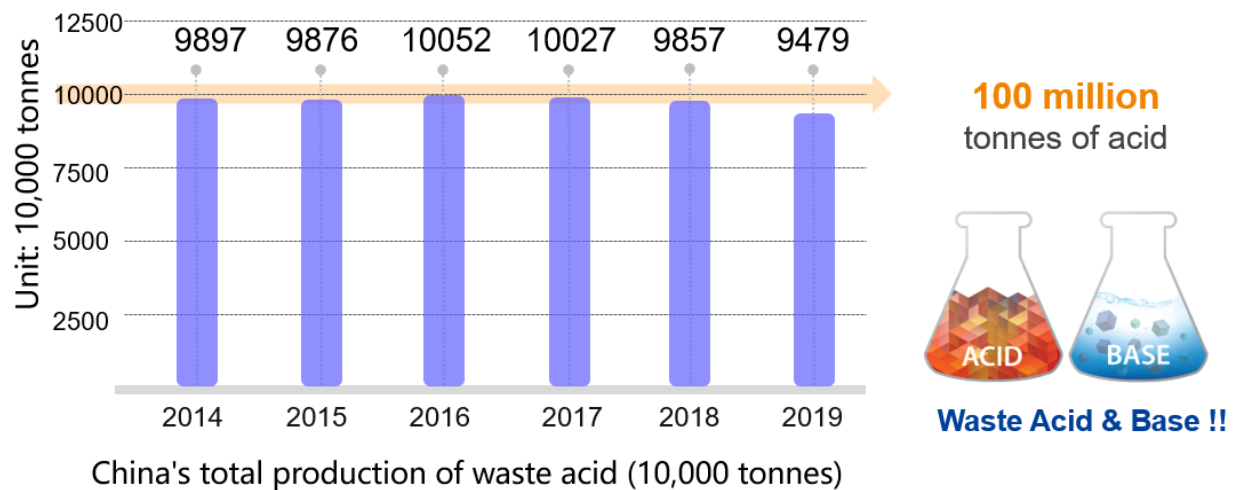


**Figure S1.** 2014-2019 China's total waste acid production statistics. Data is obtained from ref. 1.

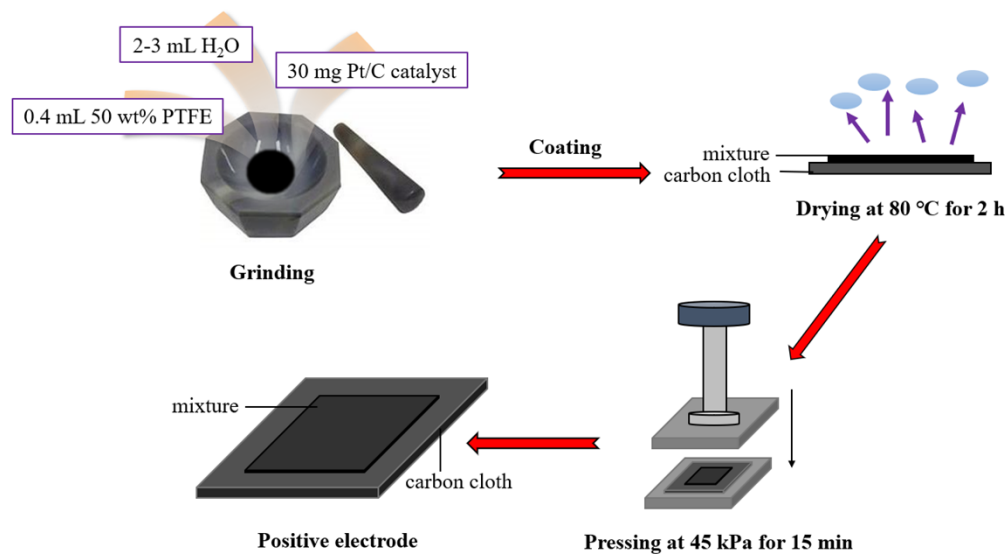


**Figure S2.** Preparation scheme of the positive electrode (i.e., the air cathode).

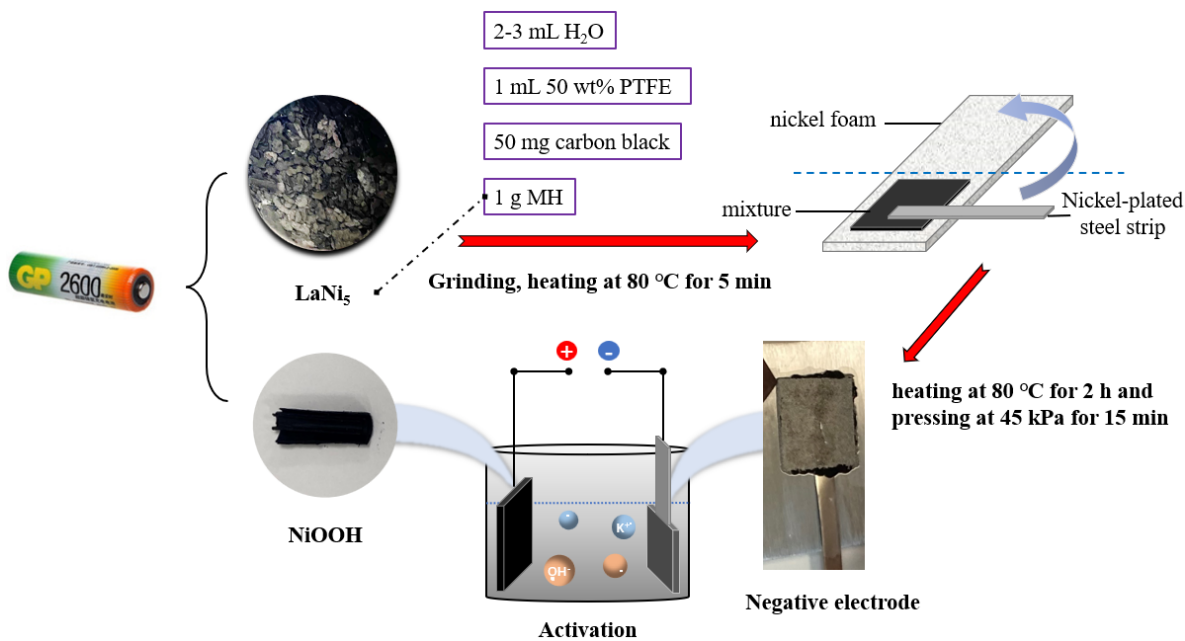


**Figure S3.** Preparation and activation schemes of the MH negative electrode.

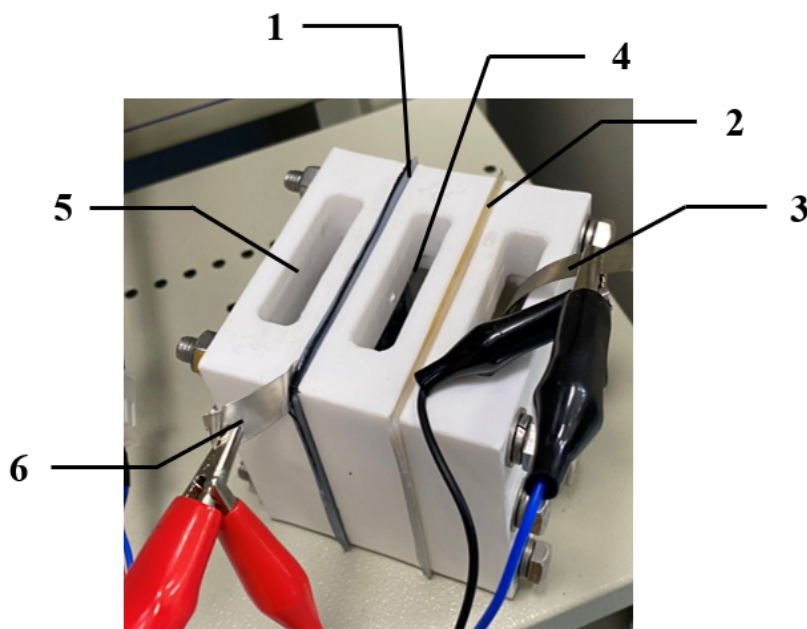


**Figure S4.** The photograph of the actual device setup. Air diffusion electrode 1, AEM 2, nickel plated steel stripped metal hydride electrode soaked in alkaline solution 3, teflon chamber with acidic solution in contact with the catalyst layer of the air diffusion electrode 4, teflon chamber allowing the gas diffusion layer of the air diffusion electrode contact with air 5, conductive stainless-steel current collector in contact with the air diffusion electrode catalyst layer 6. It is noted that the complexity of wastewater has little impact on the stability of the assembly parts.

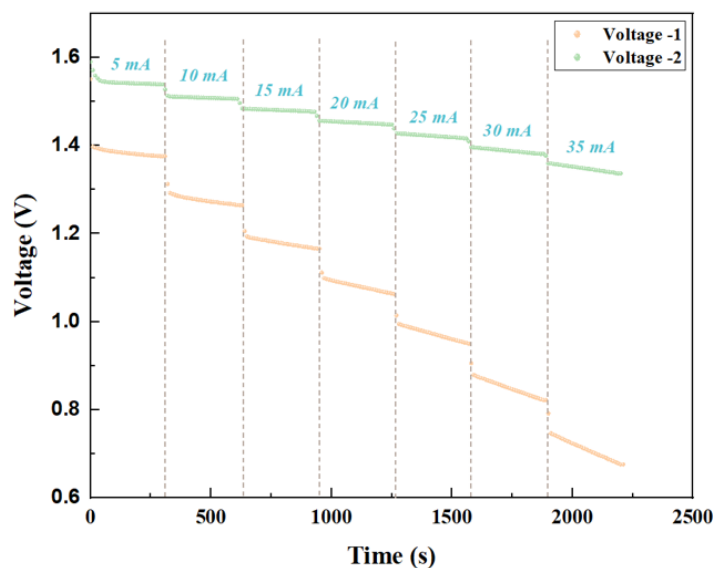


**Figure S5.** The voltage-time curves of the Air/MH batteries under different applied currents. The battery was discharged with the constant current from 5 mA to 35 mA at the intervals of 5 mA for 5 minutes. The open-circuit voltage was measured at intervals of 10 s. Voltage 1 represents the test with 0.5 mol/L H<sub>2</sub>SO<sub>4</sub> and 1 mol/L KOH, and the negative electrode was pressed at 45kPa; while Voltage 2 represents the test with 1 mol/L H<sub>2</sub>SO<sub>4</sub> and 1 mol/L KOH, and the negative electrode was pressed at 45MPa. The membrane used for both battery systems was Lanran® CEM. By comparison, the second battery is more efficient and stable since the working voltage is higher and changes slowly over time, which results from compactness of the negative electrode due to larger pressure in preparation. In general, the working voltages of both situations are relatively high, which is enough to run some small devices of low power. However, according to the measured pH values, the Coulombic efficiency was estimated to 8% and 6%, respectively. This indicates that CEM was not suited under such conditions.

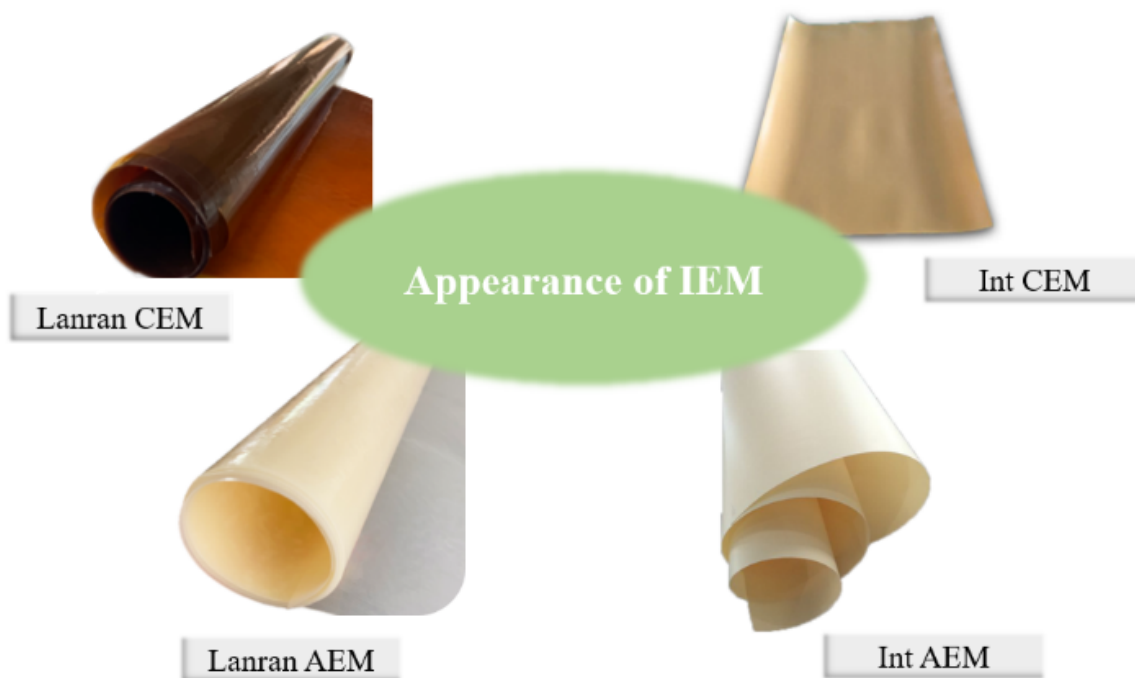


**Figure S6.** Appearance of the ion-exchange membranes for the proof-of-concept tests.

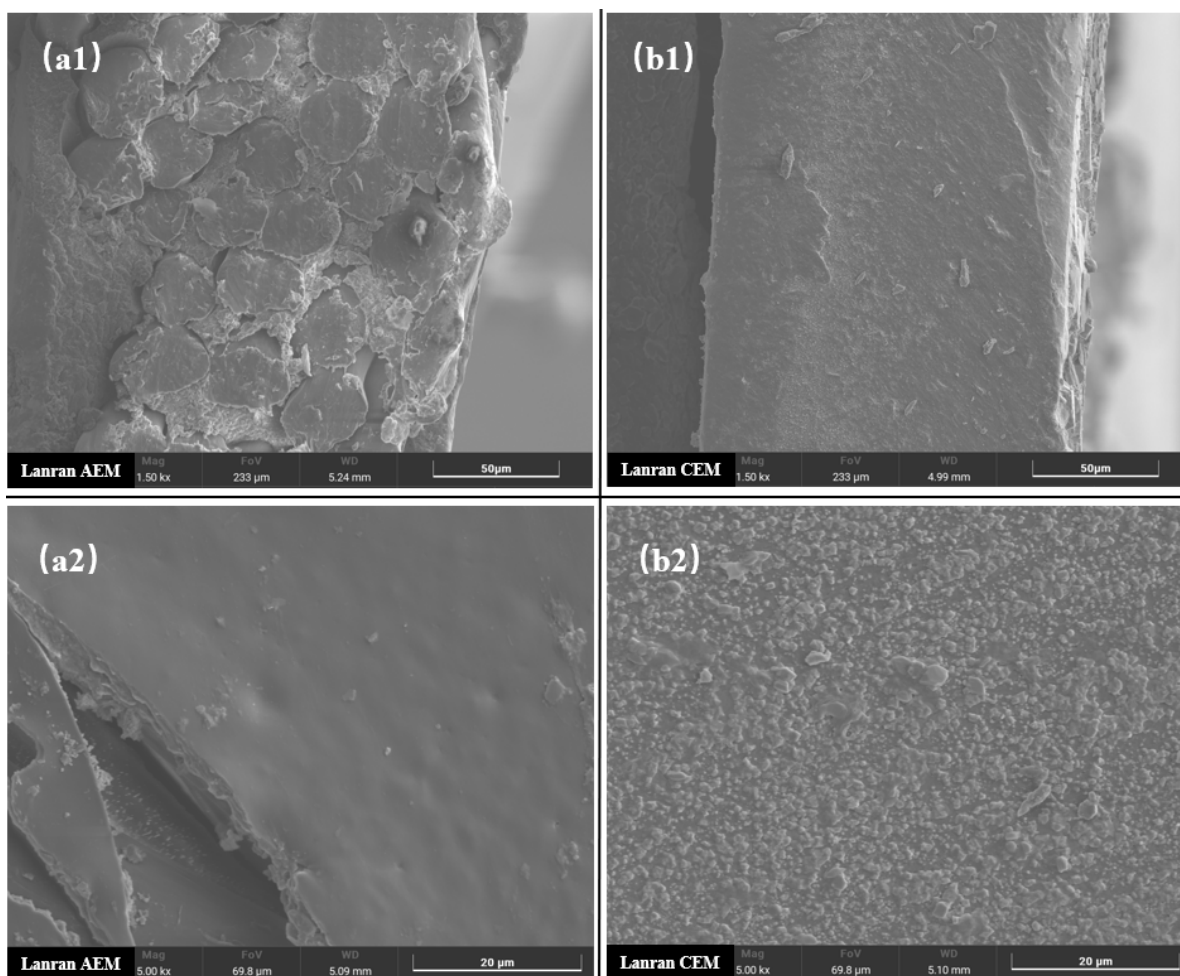


**Figure S7.** SEM images for Lanran® AEM (a1)×1.5k (a2)×5k; Lanran® CEM (b1)×1.5k (b2)×5k. (a1) and (b1) were sectional images of the membranes while (a2) and (b2) reflected the surface situation. For sectional areas, Lanran® AEM had a fibrous structure while Lanran® CEM was generally smooth and flat. For surface parts, Lanran® AEM had some tiny holes on the surface, due to which it could be assumed that Lanran® AEM had a stronger ability to absorb ions in liquid environment on account of larger specific surface area.<sup>2</sup> The white particles clung to the surface were supposed to be NaCl because there was no post-treatment when the membranes were taken out from NaCl solution. Since the number of those white particles in Figure S7 b2 was much larger than those in other figures, it could be deduced that Lanran® CEM had a stronger ability to absorb impurity like salt grains, which might decrease its exchange capacity when operating in practical waste solutions.

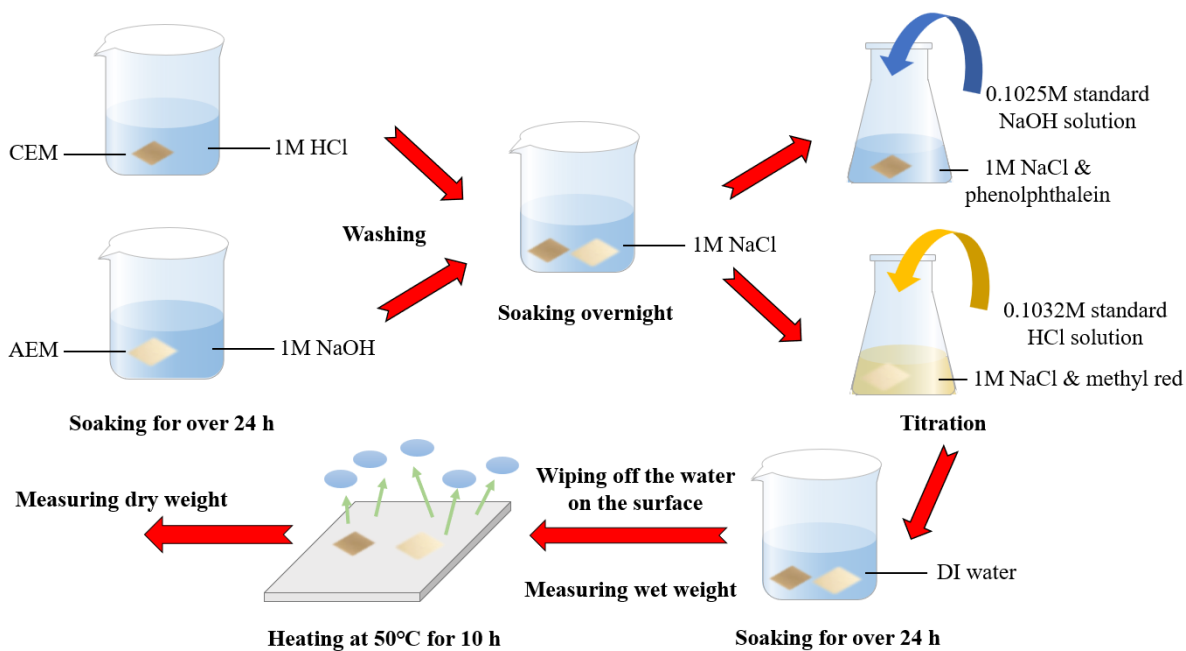


**Figure S8.** Experimental scheme for the determination of ion-exchange capacity and water uptake.

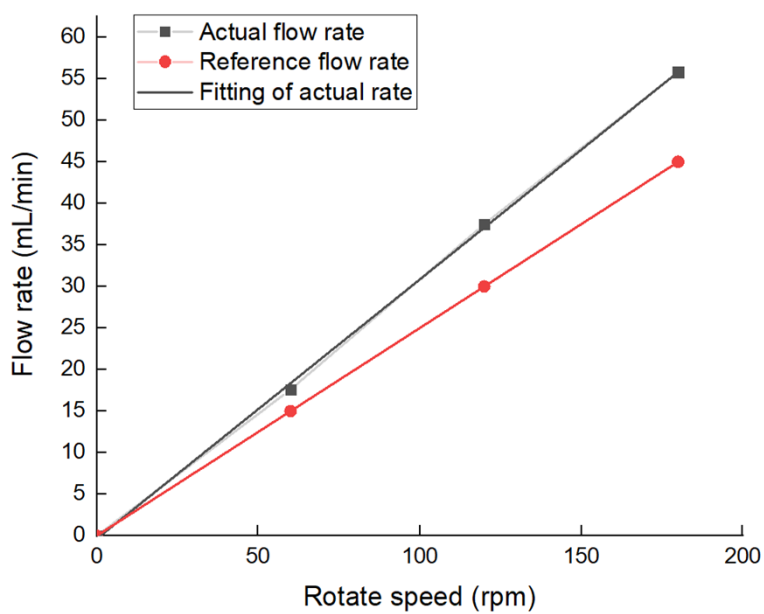


**Figure S9.** Relationship between flow rate and rotate speed of the peristaltic pump.<sup>3</sup>

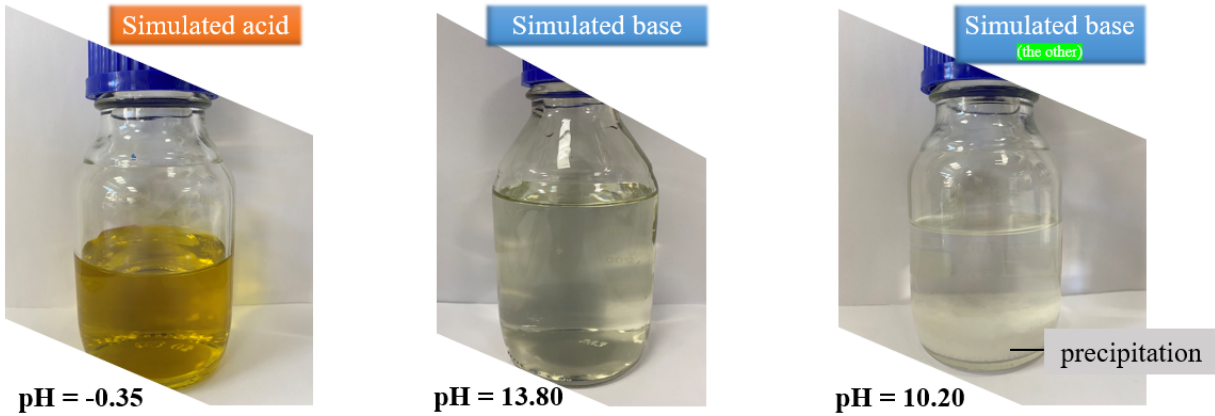


**Figure S10.** Simulated acid and base solutions for the proof-of-concept tests.

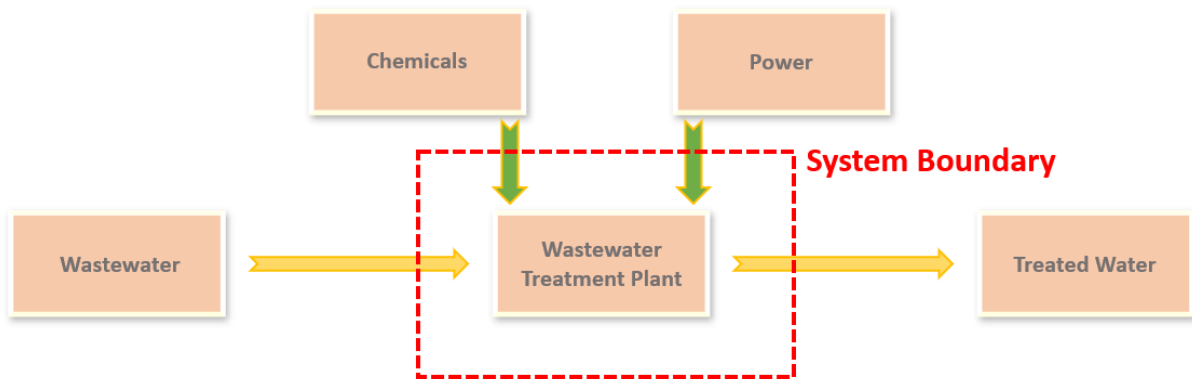


**Figure S11.** The system boundary for the wastewater treatment plant of interest, modified from the related data and information provided by PE International GmbH.



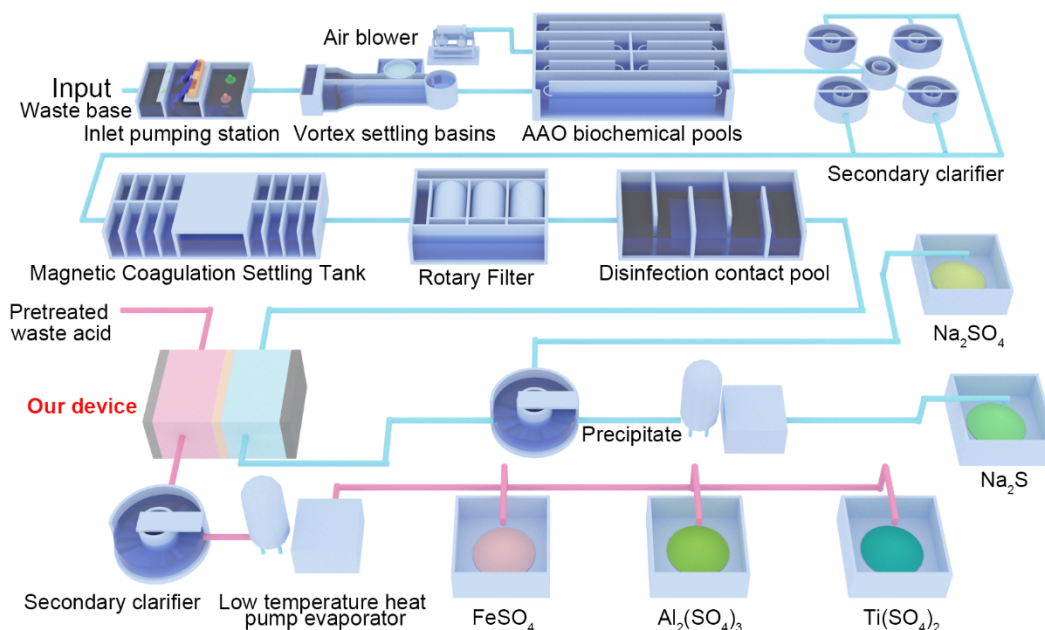


**Figure S12.** A proposed flowchart of industrial acid-base wastewater treatment process according to the information provided by Kunshan WSD Environmental Protection Equipment Co., Ltd. (located in Kunshan, Jiangsu Province, China). More details about each step are shown as follows. Vortex settling basins: separation of sand and gravel; AAO biochemical pools: degradation of organic matter; Secondary clarifier: separation of sludge from water; Magnetic coagulation settling tank: removal of tiny particles; Rotary filter: filtration; Disinfection contact pool: disinfection; Low temperature heat pump evaporator: obtaining crystals in a highly concentrated solution. Notes: The pretreated waste acid may undergo a similar pretreatment process like waste base; therefore, only the pretreatment process of waste base is specified here for the interest of simplicity. For the same reason, the separation methods of different salts are also not detailed here. Precautions should be taken when concentrated acid and base are involved. The proposed system can also exhibit an extraction effect on  $\text{SO}_4^{2-}$  ions.

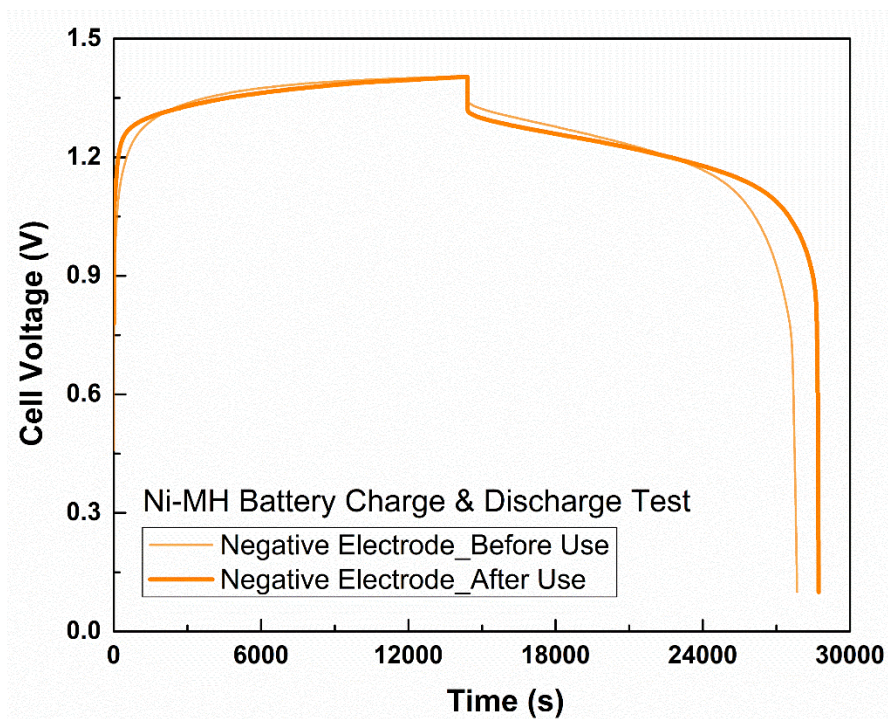


**Figure S13.** The comparison of the charge and discharge performance of the negative electrode before and after use.

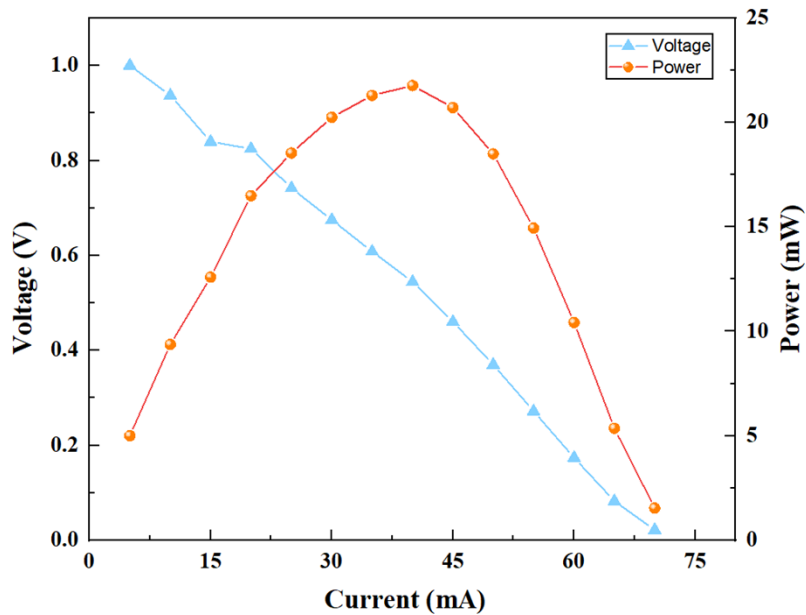


**Figure S14.** The polarization curves of the Air/MH battery using simulated acid and the other simulated base mimicked from the one produced in nickel hydrometallurgy. Lanran® AEM was used as the separator and the battery was in semi-flow mode during the test. The tested currents were from 5 mA to 70 mA to explore the universality of the proposed battery system.

**Table S1.** Composition and pH of pure and simulated electrolytes.

Electrolytes	Pure acid	Pure base	Simulated acid <sup>4</sup>	Simulated base <sup>5</sup>	Simulated base (the other) <sup>6</sup>
<i>Composition</i>	17 wt% H <sub>2</sub> SO <sub>4</sub>	7 wt% NaOH	17 wt% H <sub>2</sub> SO <sub>4</sub> 5 wt% FeSO <sub>4</sub> 1.5 wt% Al <sub>2</sub> (SO <sub>4</sub> ) <sub>3</sub> 1 wt% Ti(SO <sub>4</sub> ) <sub>2</sub>	7 wt% NaOH 0.35 wt% Na <sub>2</sub> S	3 wt% Na <sub>2</sub> CO <sub>3</sub> 0.5 wt% NaHCO <sub>3</sub> 0.1 wt% NaOH 0.5 wt% NaClO

**Table S2.** Characteristics of the commercial ion-exchange membranes.

<i>IEM</i>	Lanran® CEM <sup>7</sup>	Lanran® AEM <sup>8</sup>	Int CEM <sup>9</sup>	Int AEM <sup>10</sup>
<i>Material</i>	/	/	Gel polystyrene cross-linked with divinylbenzene	Gel polystyrene cross-linked with divinylbenzene
<i>Functional groups</i>	/	/	Sulfonic acid group	Quaternary ammonium
<i>Color</i>	Dark brown	Beige	Brown	Beige
<i>Thickness/mm</i>	0.10	0.22	0.45±0.025	0.45±0.025
<i>pH range of use</i>	0-14	0-14	1-10	1-10
<i>Resistance (Ω/cm<sup>2</sup>)</i>	3.6	4.1	<30	<40

**Table S3.** Basic properties of the commercial ion-exchange membranes.

<b>Membrane</b>	<b>Water uptake (%)</b>	<b>IEC/(meq·g<sup>-1</sup>)</b>		<b>Apparent trans. number</b>	
		Experiment	Standard <sup>9, 10</sup>	Experiment	Standard <sup>9, 10</sup>
<i>Lanran® AEM</i>	17.50	1.93	NA	0.975	NA
<i>Int AEM</i>	32.81	0.64	1.3+0.1	0.975	0.90
<i>Int CEM</i>	38.69	1.78	1.6+0.1	0.951	0.94

**Table S4.** The detailed concentration changes of different species after discharge.

Group	Species (mol/L)				
	Na	Fe	Al	S	Ti
<i>Pure base (before)</i>	1.7569	/	/	/	/
<i>Pure acid (before)</i>	/	/	/	1.7475	/
<i>Simulated base (before)</i>	1.7506	/	/	0.1069	/
<i>Simulated acid (before)</i>	0.0076	0.3716	0.0863	1.7824	0.0365
<i>Pure base (after)</i>	1.7575	/	/	0.3572	/
<i>Pure acid (after)</i>	0.0038	/	/	1.4108	/
<i>Simulated base (after)</i>	1.7506	0.0004	0.0003	0.4006	0.0002
<i>Simulated acid (after)</i>	0.0022	0.3443	0.0813	1.4368	0.034

**Table S5.** The mean titration results of the initial and treated base solutions.

	2 mL Initial base	2 mL Treated base
<i>Volume of consumed 1/2 H<sub>2</sub>SO<sub>4</sub></i>	31.75 mL	8.56 mL

**Table S6.** The impact categories and their units of the selected LCIA method of the project.

<b>Indicator</b>	<b>Unit</b>
Aquatic acidification	kg SO <sub>2</sub> eq
Global warming	kg CO <sub>2</sub> eq
Ionizing radiation	Bq C-14 eq
Land occupation	m <sup>2</sup> org.arable
Mineral extraction	MJ surplus
Non-renewable energy	MJ primary
Ozone layer depletion	kg CFC-11 eq
Respiratory inorganics	kg PM <sub>2.5</sub> eq
Respiratory organics	kg C <sub>2</sub> H <sub>4</sub> eq
Terrestrial acid/nutri	kg SO <sub>2</sub> eq
Terrestrial ecotoxicity	kg TEG soil

**Table S7.** The detailed impact assessment results of the different project variants.

<b>Indicator</b>	<b>The plant with power generation</b>	<b>The plant without power generation</b>
Aquatic acidification	$1.95969 \times 10^{-5}$	$5.19759 \times 10^{-5}$
Global warming	$3.49953 \times 10^{-3}$	$1.42166 \times 10^{-2}$
Ionizing radiation	$8.03698 \times 10^{-3}$	$3.26498 \times 10^{-2}$
Land occupation	$5.00041 \times 10^{-7}$	$2.03139 \times 10^{-6}$
Mineral extraction	$2.28464 \times 10^{-8}$	$9.28125 \times 10^{-8}$
Non-renewable energy	$4.72558 \times 10^{-2}$	$1.91975 \times 10^{-1}$
Ozone layer depletion	$7.06982 \times 10^{-11}$	$2.87208 \times 10^{-10}$
Respiratory inorganics	$1.36509 \times 10^{-6}$	$5.54563 \times 10^{-6}$
Respiratory organics	$3.67950 \times 10^{-7}$	$1.49478 \times 10^{-6}$
Terrestrial acid/nutri	$4.11630 \times 10^{-5}$	$1.67223 \times 10^{-4}$
Terrestrial ecotoxicity	$1.95474 \times 10^{-3}$	$7.94071 \times 10^{-3}$



## Supplementary Note S1

Here a brief overview of the waste acid-base treatment methods is provided. At present, the waste acid and base have been mainly treated by chemical neutralization both in China<sup>11</sup> and overseas<sup>12, 13</sup>. Biotechnology has also been used to treat acid-base waste solutions containing high-concentrated organic matters and sulfur-based species.<sup>14, 15</sup> In addition to these commonly used methods, there have been some other special conventional technologies of dealing with waste acid and base in China and overseas. Some of the typical ones are shown below.

High temperature incineration:

Since pH can be adjusted by neutralization between acid and base, how to deal with the organic impurities and recycle the useful matters has become a problem. High temperature incineration provides a method to solve it.<sup>16</sup> After reasonable pretreatment, the waste acid and base are sprayed into the cement kiln and destroyed at high temperature. At the same time, it is mixed with waste mineral oil, waste emulsified oil, waste cleaning agent, waste organic solvent, etc. to make it have a certain calorific value, and it is incinerated and destroyed in a cement kiln. Afterwards, liquid waste obtained can be used to produce cement. The detailed procedures are shown as follows:

- (1) Under normal pressure, in the pretreatment center, neutralize the waste acid liquid and waste lye with agitator in the neutralization tank, and the reaction temperature is controlled at 20 °C-95 °C.
- (2) When neutralizing, according to the different pH, calcium hydroxide solution or waste acid is added through the acid and base adding device, so that the treated industrial waste liquid has weak alkalinity, and the pH value is controlled at 8-10.
- (3) The waste liquid after neutralization reaction is transferred to the plate and frame filter press which is carried out under the working pressure of 10 to 14 MPa. After the pressure filtration, the

liquid enters the liquid waste storage tank, and the solid is transferred to the solid waste pretreatment center.

(4) The waste liquid after the neutralization reaction is mixed with waste mineral oil, waste emulsified oil, waste cleaning agent, waste organic solvent, etc. under the condition that no adverse reactions and dangerous substances are produced, and the calorific value of the waste liquid is adjusted so that the final heat value of the prepared industrial waste liquid is 2400 kJ/kg to 20000 kJ/kg.

(5) The liquid waste after adjusting the calorific value is pumped to the high-level storage tank on the top of the tower at the end of the furnace, and injected into the cement rotary kiln through the spray gun of the kiln head burner for incineration. When producing cement, the temperature of the kiln head gas stabilized at 1750 °C.

The characteristics of the treated waste solution are: i) using the rotary kiln to incinerate the industrial waste solution; ii) using the pump force to transport and directly spray into the new rotary incinerator through the multi-channel burner and can realize the complete incineration treatment; iii) the process is continuous, automatic, safe and reliable, no secondary pollution. The organic matter in the waste solution is completely incinerated at high temperature, and a small amount of inorganic matter contained in the waste solution is used as raw material for cement production, and finally enters cement products.

Synthesis of useful materials:

Waste acid and base as raw material to produce chemical products such as polyferric aluminum chloride.<sup>17</sup> Use pickling waste liquid from steel mills (generally a large amount) and mechanical processing industry scrap iron as raw materials to prepare polymeric iron-aluminum coagulant (PFAC), and use aluminum products to process alkali-washed aluminum-containing waste

solution (generally small amount). Adjust its salinity so that waste acid and alkali can be utilized at the same time. Membrane technology can be used to recycle or regenerate waste solution.<sup>18, 19</sup> However, the investment in membrane treatment equipment is high, and the high concentration of waste acid and lye has high requirements on the membrane itself and its equipment, which increases the treatment cost.

Bipolar membrane treatment:

In foreign countries, wet oxidation has been used to treat waste alkali liquor, and bipolar membrane has been used to regulate the conversion of chemical neutralization energy into electrical energy.<sup>20,</sup>

<sup>21</sup> The cation exchange membrane is a selective barrier separating the anode and cathode compartments, whose role is to be selectively permeable to cations, preferably protons moving from the anode to the cathode. For the anion exchange membrane, it is selectively permeable to anions. Composed by a cation exchange layer and an anion exchange layer, bipolar membranes (allowing the generation of protons and hydroxide ions via a water dissociation mechanism) are connected by a catalytic interlayer and are usually adopted to regenerate acid and base solutions from a salt stream by the Bipolar Membrane Electrodialysis (BMED) process<sup>22, 23</sup> via water dissociation ( $\text{H}_2\text{O} \rightarrow \text{H}^+ + \text{OH}^-$ ) under an applied electric field. Bipolar Membrane Reverse Electrodialysis (BMRED) is the reverse process, which allows energy to be produced by controlling the mixing of acid and base solutions. The working principle of BMRED is similar to that of conventional Reverse Electrodialysis.<sup>24</sup> It relies on the electrical potential provided by the concentration gradient between two solutions on each side of the membrane. However, due to the risk of membrane delamination which can strongly limit the process performance, it has not been put into large-scale industrial production and treatment.<sup>23</sup> In fact, all of today's available electro-membrane processes and components used in these processes still have technical and commercial

limitations and in spite of a substantial ongoing development there is a need for further research to improve products and processes.<sup>25</sup>

### Supplementary Note S2

Ion-exchange capacity (IEC) was measured using a titration method (Figure S11).<sup>26</sup> All IEMs were cut to size of 1×1 cm<sup>2</sup>, respectively. The cation-exchange membrane (CEM) was firstly soaked in 1 mol/L HCl (diluted from 36% HCl, Sinopharm) while the anion-exchange membrane (AEM) was soaked in 1 mol/L NaOH (prepared using NaOH flaky solid, Sinopharm AR, ≥99.5%) for over 24h. Then they were washed with DI water to remove excess HCl and NaOH and were subsequently immersed into 1 mol/L NaCl solution (prepared using NaCl solid, Sinopharm AR, ≥99.5%) overnight. For CEM, the number of displaced protons from the membrane was determined by titration with 0.1025 M standard NaOH solution (Sinopharm AR) using phenolphthalein (Sinopharm Ind) as the indicator; For AEM, the number was determined with 0.1032 M standard HCl solution (Sinopharm AR) indicated by methyl red (Aladdin). After that, the membranes were soaked in DI water for over 24h and then taken out with water on the surface wiped off using tissue paper. The wet weight of membrane was measured. Next, the membranes were placed in an oven at 50 °C for 10 h or more until there was no change in weight. The dry weight of membrane was recorded. The IEC and water uptake of membranes were calculated by Eqns. S1 and S2.

$$IEC = \frac{ab}{W_{dry}} \quad (S1)$$

$$Water\ uptake\% = \frac{W_{wet} - W_{dry}}{W_{dry}} \times 100\% \quad (S2)$$

where  $a$  is the concentration of NaOH solution or HCl solution used (mol/dm<sup>3</sup> or M),  $b$  is the volume of NaOH or HCl solution used (dm<sup>3</sup>),  $W_{\text{dry}}$  is the dry weight of the membrane and  $W_{\text{wet}}$  is the wet weight of the membrane.

Transport number is basic in determining the efficiency of electro-membrane separation processes, is related with membrane potential.<sup>27</sup> To obtain those two significant parameters, membranes were tested in static state and stirring state respectively. For the static state, membrane potential was measured in a two-compartment cell, in which a vertical membrane of 1.0 cm<sup>2</sup> effective area separated two solutions of 0.01 mol dm<sup>-3</sup> NaCl and 0.05 mol dm<sup>-3</sup> NaCl, respectively. The potential difference across the membrane was measured using a multimeter which was connected to Ag/AgCl reference electrodes. For the stirring state, the only difference was that while testing the membrane transport number, both the solutions were continuously stirred. The apparent transport number,  $\bar{t}_+$ , was calculated by the following Eqn. S3:

$$E_m = \frac{RT}{F} (2\bar{t}_+ - 1) \ln \left( \frac{C_1}{C_2} \right) \quad (\text{S3})$$

where  $R$  is the gas constant (J/(mol·K)),  $F$  is the Faraday constant (C/mol),  $T$  is the absolute temperature (K),  $C_1$  and  $C_2$  are the concentration (mol/dm<sup>3</sup> or M) of electrolyte solutions in the testing cell.

Water uptake and IEC are significant determinant of water and salt permeability and salt diffusion coefficients for ion exchange membranes.<sup>28</sup> Together with transport number, they were examined as the major characteristics of IEM (Table S7).<sup>29</sup> Lanran® AEM has the smallest water uptake, which indicates that when placed into the solution it swells the least and poses little damage to the whole structure of the device. The materials on the surface are the most hydrophobic. It also has the largest IEC and transport number, producing weaker barrier to the ion movement and

consequently possesses the lowest resistance, which could improve the performance of the battery. By comparison, Int AEM and CEM have weaker selection of specific ion to flow through due to the relatively simple structure of the membranes while complicated fibrous structure in Lanran® AEM sets more obstacles for positively-charged ions. Both the numerous tiny holes on the surface and larger specific area of Lanran® AEM could be helpful to improve the ion exchange capacity and transport number, allowing more ions to pass through the surface in a short period of time.

### **Supplementary Note S3**

An interesting phenomenon occurred during discharging process of the fully charged MH electrode within the Air/MH battery was that a lot of white bubbles or gas bubbles appeared on the surface of negative electrolyte if the electrolyte concentration of the activation cell was different to that of the Air/MH cell, possibly resulting from imbalanced concentration difference. When the negative electrode was fully charged in 4 wt% NaOH solution, the hydrogen stored inside metal hydride was in balance with ions in the solution. However, when the electrode was soaked in higher concentration environment (7 wt% NaOH), larger pressure difference led to the automatic release of hydrogen (i.e., white or gas bubbles) from the negative electrode, affecting the overall performance of the Air/MH battery. Therefore, 7 wt% NaOH, whose concentration was the same as that in the simulated waste base solutions, was selected to serve as the charging base solution.

### **Supplementary Note S4**

The title of the data set used in this work is “waste water treatment, at waste water treatment plant, chemical reduction/oxidation process, municipal waste water (copy)”. This data set represents an

average waste water treatment plant using the chemical reduction/oxidation process. Inputs to the process are: waste water untreated, iron chloride, hydrated lime (dry slaked), phosphoric acid, power and thermal energy from natural gas. Here, the required power and heat for this system are probably produced from natural gas turbine. In other words, co-generation from natural gas is involved. Notes: Co-generation, or combined heat and power (CHP), is the simultaneous production of electricity and useful heat, which has been widely applied to improve energy efficiency and enjoy low-carbon benefits.<sup>30</sup> Moreover, co-generation based on renewables, especially those (e.g., solar and geothermal resources) generate electricity via prior thermal generation, can lead to the supply of very low-carbon electricity and heat.<sup>30</sup> Should the power generation from the neutralization reaction via Air/MH battery is used, the energy required for the treatment plant can be reduced. The outputs are treated water and the emissions to fresh water. Emissions are calculated based on the reduction number provided by the user in the variable parameters. Energy supply chain and the production of intermediates used in the process are not included in the data set. Data set valid for annually equal discharge. Not appropriate for differences in seasons or seasonal peaks. Average based on Central European countries. No distinction between Northern and Southern Europe is done. The above information is mostly quoted from the OpenLCA database for an explicit description.

## References

1. Report of products and investment strategy planning analysis on China waste acid recovery industry, Accessed on May 7<sup>th</sup> 2023. (ed<sup>^</sup>(eds) (2020).
2. Matsumoto H, Tanioka A. Functionality in Electrospun Nanofibrous Membranes Based on Fiber's Size, Surface Area, and Molecular Orientation. *Membranes* **1**, 249-264 (2011).

3. *Peristaltic pump (LongerPump, WT600-2J, YZ1515x) hose pump head flow conversion*  
URL: <https://www.longerpump.com.cn/index.php/PeristalticPumpTechnique/show/22.html>.
4. Treatment of Wastewater in Titanium Dioxide Production[EB/OL]. (2012-11-05) [2023-05-07] <https://www.docin.com/p-517123865.html>.
5. 余政哲, 孙德智, 郭宝珠, 李长海, 史鹏飞. 均相化学催化氧化法处理废碱液中硫化物的研究. *西安石油大学学报(自然科学版)* **19**, 63-65 (2004). Yu Zhengzhe, Sun Dezhi, Guo Baozhu, Li Changhai, Shi Pengfei. Study on the treatment of sulfides in waste lye by homogeneous chemical catalytic oxidation. *Journal of Xi 'an Shiyou University (Natural Science Edition)* **19**, 63-65 (2004).
6. 冯拥军. 硫酸尾气碱性废水脱硫的研究与实践. *硫酸工业*, 3 (2013). Feng Yong-Jun. Research and practice on desulfurization of sulfuric acid tail gas alkaline wastewater. *Sulfuric Acid Industry*, 3 (2013)
7. CEM-CT-4, Lanran[EB/OL]. (2022-05-15) [2023-05-07]  
[http://www.lanran.com.cn/?list\\_8/105.htm](http://www.lanran.com.cn/?list_8/105.htm) l.
8. AEM-AHT, Lanran[EB/OL]. (2022-05-15) [2023-05-07]  
[http://www.lanran.com.cn/?list\\_8/102.htm](http://www.lanran.com.cn/?list_8/102.htm) l.
9. CMI-7000S, a non-reinforced cation exchange membrane (CEM)[EB/OL]. (2020-05-12) [2023-05-07] <http://en.scimaterials.cn/ProDetail.aspx?ProId=513>.
10. AMI-7001S, a non-reinforced anion exchange membrane (AEM)[EB/OL]. (2020-05-12) [2023-05-07] <http://en.scimaterials.cn/ProDetail.aspx?ProId=506>.
11. 马小乐, 霍佳梅, 董四禄. 铜冶炼废酸处理工艺设计. *硫酸工业*, 5 (2019). Ma Xiaole, Huo Jiamei, Dong Silu. Design of waste acid treatment process for copper smelting. *Sulfuric Acid Industry*, 5 (2019).
12. Petruzzelli D, Petrella M, Boghetich G, Calabrese P, Petruzzelli V, Petrella A. Neutralization of Acidic Wastewater by the Use of Waste Limestone from the Marble Industry. Mechanistic Aspects and Mass Transfer Phenomena of the AcidBase Reaction at the LiquidSolid Interface. *Indengchemres* **48**, 399-405 (2009).
13. Goel RK, Flora JRV, Chen JP. Flow Equalization and Neutralization, Part of the Handbook of Environmental Engineering book series (HEE, volume 3). (2005).



14. 郝玉翠, *et al.* 生物强化技术处理碱渣废水工程实例. *石油化工安全环保技术* **33**, 5 (2017). Hao Yucui, *et al.* A case study of alkaline sludge wastewater treatment by bioenhancement technology. *Petrochemical safety and environmental protection technology* 33, 5 (2017).
15. 李红政. 含高浓度有机物废酸碱中和处理技术. 山东省, 山东国标环境工程有限公司, (2017-04-01). Li Hongzheng. Neutralization technology of waste acid and alkali containing high concentration organic matter. Shandong, Shandong National Standard Environmental Engineering Co., LTD., (2017-04-01).
16. *工业废液处理方法[J]技术与市场,2007(02):14.* Treatment of industrial waste liquid [J] *Technology and Market,2007(02):14.*
17. 邵青, 霍文敏, 苑运丽, 王震. 以废酸、废碱液制备聚合氯化铁铝的实验研究. *工业水处理* **32**, 4 (2012). Shao Qing, Huo Wenmin, Yuan Yunli, Wang Zhen. Experimental study on preparation of polyferric aluminum chloride from waste acid and waste lye. *Industrial Water Treatment* 32, 4 (2012).
18. Schmidt B, *et al.* Rinse water regeneration in stainless steel pickling. *Desalination* **211**, 64-71 (2007).
19. Regel-Rosocka M. A review on methods of regeneration of spent pickling solutions from steel processing. *Journal of hazardous materials* **177**, 57-69 (2010).
20. Y. Z. Wet oxidation technology based on organic wastewater treatment. *Journal of Physics: Conference Series* **1549**, 022040 (2020).
21. Zaffora A, Culcasi A, Gurreri L, Cosenza A, Micale G. Energy Harvesting by Waste Acid/Base Neutralization via Bipolar Membrane Reverse Electrodialysis. *Energies* **13**, 5510 (2020).
22. And CH, Xu T. Electrodialysis with Bipolar Membranes for Sustainable Development. *Environ Sci Technol* **40**, 5233–5243 (2006).
23. Thiel GP, Kumar A, Gómez-González A, Lienhard JH. Utilization of Desalination Brine for Sodium Hydroxide Production: Technologies, Engineering Principles, Recovery Limits, and Future Directions. *Acs Sustainable Chemistry & Engineering* **5**, 11147–11162 (2017).

24. Hong JG, *et al.* Potential ion exchange membranes and system performance in reverse electro dialysis for power generation: A review. *Journal of Membrane Science* **486**, 71-88 (2015).
25. Strathmann H. Electrodialysis, a mature technology with a multitude of new applications. *Desalination* **264**, 268–288 (2010).
26. Klaysom C, Moon SH, Ladewig BP, Lu GQM, Wang L. Preparation of porous ion-exchange membranes (IEMs) and their characterizations. *Journal of Membrane Science* **371**, 37-44 (2011).
27. Koter S. Transport number of counterions in ion-exchange membranes. *Separation & Purification Technology* **22**, 643-654 (2001).
28. Kingsbury RS, Bruning K, Zhu S, Flotron S, Coronell O. Influence of Water Uptake, Charge, Manning Parameter, and Contact Angle on Water and Salt Transport in Commercial Ion Exchange Membranes. *Industrial & Engineering Chemistry Research* **58**, 18663-18674 (2019).
29. Yoon H, Jo K, Kim KJ, Yoon J. Effects of characteristics of cation exchange membrane on desalination performance of membrane capacitive deionization. *Desalination* **458**, 116-121 (2019).
30. Veerapen J, Beerepoot M. Co-generation and Renewables: Solutions for a low-carbon energy future. Accessed on May 10th 2024. (ed^(eds). International Energy Agency (2011).